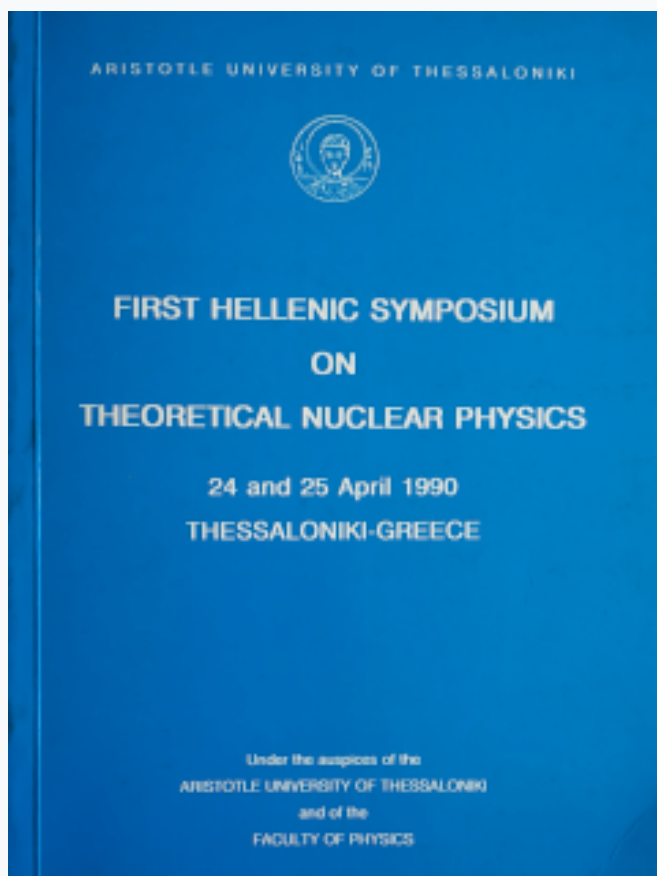


HNPS Advances in Nuclear Physics

Vol 1 (1990)

HNPS1990



Effective interactions in the sd and p shells

J. C. Varvitsiotis, L. D. Skouras

doi: [10.12681/hnps.2835](https://doi.org/10.12681/hnps.2835)

To cite this article:

Varvitsiotis, J. C., & Skouras, L. D. (2020). Effective interactions in the sd and p shells. *HNPS Advances in Nuclear Physics*, 1, 168–178. <https://doi.org/10.12681/hnps.2835>

J.C. Varvitsiotis and L.D. Skouras

Institute of Nuclear Physics, N.C.S.R. Demokritos, Aghia Paraskevi GR 15310, Greece

ABSTRACT: Using matrix-inversion techniques effective interactions for the sd and p shells are determined in the complete space $0\hbar\omega + 2\hbar\omega$. The derived interactions are used to determine the spectra of $A=18-20$ and $A=5-15$ nuclei and compare them with experiment.

1. INTRODUCTION

One of the purposes of nuclear theory is the derivation of effective interactions appropriate for shell model calculations. Since the pioneer work of Kuo and Brown (1966), there has been a large amount of studies in this field trying to deduce effective interactions using several methods and techniques.

In this paper, we describe a method based on matrix-inversion techniques to derive effective interactions appropriate for shell model calculations in the sd and p shells (Skouras and Varvitsiotis 1990a,b). In this method the energy matrices are constructed in the space of $0\hbar\omega + 2\hbar\omega$ excitations and convergence studies are made for the effective interaction after the elimination of the unlinked graphs in the above space.

This work falls in three parts. First, the elimination of unlinked graphs in the space of $0\hbar\omega + 2\hbar\omega$ excitations is shown in sect.2, which leads to the linked plus folded diagram expansion. The summation of the above expansion is performed in sect.3 and finally the results of the calculation are given in sect.4.

2. ELIMINATION OF UNLINKED DIAGRAMS IN $0\hbar\omega + 2\hbar\omega$ SPACE

The energy matrices are constructed for the $A=16-18$ and $A=4-8$, $A=14-16$ systems in a space that includes all $0\hbar\omega + 2\hbar\omega$ excitations. The Hamiltonian for a system of A nucleons has the form

$$H = \sum_{i=1}^A t_i + \sum_{i<j}^A V(i, j) \quad (1)$$

¹ Presented by J.C. Varvitsiotis

where t denotes the kinetic energy, V the two body interaction while A the number of the nucleons in the nucleus. The Hamiltonian (1) can be written as

$$H = H_0 + H_1 \quad (2)$$

where

$$H_0 = \sum_{i=1}^A (t_i + U_i), \quad H_1 = \sum_{\langle i,j \rangle} V(i,j) - \sum_{i=1}^A U(i) \quad (3)$$

and U an one body potential. We also define the projection operators

$$P = \sum_{\alpha=1}^{\mu} |\alpha\rangle\langle\alpha|, \quad Q = \sum_{i=1}^M |i\rangle\langle i|, \quad (4)$$

where P projects onto the $0\hbar\omega$ model space while Q onto the $2\hbar\omega$ space. By Greek letters $\alpha, \beta, \gamma, \dots$ are labeled the model space states while by i, j, k, \dots the $2\hbar\omega$ states. μ, M denote the dimensions of the $0\hbar\omega$ and $2\hbar\omega$ spaces respectively.

We consider now the Rayleigh-Schroedinger expansion for a degenerate system

$$V_{ij}^{r,s} = \sum_{k=1}^{\infty} S_k \quad (5)$$

Since all energy denominators in the calculation are equal, the first few terms of the above series are written as

$$S_1 = E_1 \quad (6a)$$

$$S_2 = E_2 \quad (6b)$$

$$S_3 = E_3 \quad (6c)$$

$$S_4 = E_4 - \frac{2E_3E_1}{D} + \frac{E_2E_1^2}{D^2} - \frac{E_2^2}{D} \quad (6d)$$

e.t.c, where

$$E_1 = PH_1P, \quad E_n = \frac{PH_1Q(QH_1Q)^{n-2}QH_1P}{D^{n-1}}, \quad n \geq 2, \quad D = E_0 - E_Q \quad (6e)$$

The terms of the Rayleigh-Schroedinger series (5) that produce unlinked diagrams in a space restricted to $2\hbar\omega$ excitations appear in fourth and higher orders and are those that contain two or more factors E_k with $k > 1$ (Mavromatis and Skouras 1979, Skouras and Varvitsiotis 1990a,b). For example, the term $-E_2^2/D$ of the fourth order in a double closed shell system contains the product graphs of fig.1

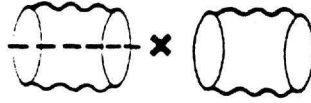


Fig. 1 Product graphs contained in $-E_2^2/D$ term of fourth-order. The dash line denotes a minus and an extra denominator D .

which in a complete space calculation are canceled by the unlinked graphs of fig.2.



Fig. 2 Fourth-order unlinked diagrams that appear in the closed core system.

The graphs of fig.2 are coming from the leading term E_4 of (6d) and don't appear in the present calculation since they involve higher than $0\hbar\omega + 2\hbar\omega$ excitations. By removing from Rayleigh-Schroedinger expansion (5) all the terms that contain more than one factor E_k with $k > 1$, the series

$$Y = \sum_{k=0}^{\infty} Y_{k+2} \quad (7)$$

results, where

$$Y_2 = E_2 \quad (8a)$$

$$Y_3 = E_3 - \frac{E_2 E_1}{D} \quad (8b)$$

$$Y_4 = E_4 - \frac{2E_3 E_1}{D} + \frac{E_2 E_1^2}{D^2} \quad (8c)$$

e.t.c. Hence, the series (7) in the $0\hbar\omega + 2\hbar\omega$ space includes only linked graphs in agreement with the formal theory of effective interactions (Brandow 1967). The summation of series (7) in the above space is the subject of the next section.

3. SUMMATION OF LINKED PLUS FOLDED DIAGRAM EXPANSION IN $0\hbar\omega + 2\hbar\omega$ SPACE

A summation to all orders of expansion (7) is obtained in a space that is the direct product of the P and Q spaces of sect.2. This space denoted by $P \otimes Q$ has dimension $\mu \times M$ and the following quantities are defined into it

a) An operator Z:

$$Z_{i\alpha, j\beta} = \frac{(QH_1Q)_{ij}\delta_{\alpha\beta} - (PH_1P)_{\alpha\beta}\delta_{ij}}{D} \quad (9)$$

b) The μ^2 row vectors Ψ_β^α ($\alpha, \beta = 1, 2, \dots, \mu$):

$$(\Psi_\beta^\alpha)_{i\gamma} = \delta_{\beta\gamma}(PH_1Q)_{\alpha i} \quad (10)$$

c) The column vector Φ :

$$\Phi_{i\gamma} = (QH_1P)_{i\gamma} \quad (11)$$

We also define the model space quantities

$$(R_n)_{\alpha\beta} = \frac{(-)^n}{D^{n+1}} \Psi_\beta^\alpha (I - Z)^{-(n+1)} \Phi, \quad n = 0, 1, 2, \dots \quad (12)$$

where I denotes the unit matrix in the $P \otimes Q$ space. The quantities R_n can be expressed in the form of a series:

$$R_n = \frac{(-)^n}{D^n} \sum_{l=0}^{\infty} \binom{n+l}{n} Y_{l+2}, \quad n = 0, 1, 2, \dots \quad (13)$$

where

$$(Y_{l+2})_{\alpha\beta} = \frac{\Psi_\beta^\alpha Z^l \Phi}{D} \quad (14)$$

The quantities R_n are the basic units in our method to derive the effective interaction. For a Q space restricted to $0\hbar\omega + 2\hbar\omega$ excitations, each R_n includes linked plus folded valence diagrams and linked core diagrams (Skouras and Varvitsiotis 1990a). By considering the difference

$$r_n^j = R_n^j - R_n^c \quad (15)$$

we obtain the valence one-body graphs, where j and c denote an orbital in the model space of ^{17}O and the core state respectively. For the two-particle system, we obtain the valence graphs by considering

$$\langle ij; JT | r_n | kl; JT \rangle = \langle ij; JT | R_n | kl; JT \rangle - \delta_{ik} \delta_{jl} (r_n^i + r_n^j + R_n^c) \quad (16)$$

where i, j, k and l denote orbitals of the sd shell.

We correspond now the quantity r_0 to the Q-box of Krenciglowa and Kuo (1974) and the quantities r_n ($n > 0$) as the derivatives of the Q-box. Hence, the effective interaction is given by the expansion

$$V_{eff} = F_0 + F_1 + F_2 + \dots \quad (17)$$

where

$$F_0 = r_0, \quad F_1 = r_1 r_0, \quad F_2 = r_2 r_0^2 + r_1^2 r_0, \quad e.t.c \quad (18)$$

4. RESULTS

In this section we present the results for the effective interactions for the sd and p shells using the method of sect.3. The results for the sd shell have been obtained with the choice of 1.7 fm for the oscillator parameter ($\hbar\omega = 14.42 \text{ Mev}$) and using for the two body interaction V in (1) the "Sussex" matrix elements of Elliot et al (1968). At first, we have to determine the quantities R_n defined in (12). As (12) shows, the exact determination of these quantities involves the inversion of matrix Z . However, the dimension of Z , as for example in the $(J,T)=(2,1)$ state of $A=18$ with dimension 17880, exceeds in several cases the capabilities of our computing system. Hence, we determine the quantities R_n approximately by summing the first fifty terms of expansion (13) in all cases where matrix inversion is not possible.

The next step contains the calculation of the operators F_n defined by (18) and the convergence study of expansion (17). The results are shown in table 1 for ^{17}O and the $J=0$ state of ^{18}O and contain contributions up to F_6 term. In table 1 the results for ^{17}O include the zero-order contribution and give the energies of ^{17}O states relative to ^{16}O . The energy of ^{16}O is also included in table 1 calculated by considering only the contribution of F_0 term. As it is clear from table 1, for the ^{17}O case there is a rapid convergence of expansion (17). Hence, the energy of ^{17}O states is almost completely attributed by the first two terms F_0 and F_1 . In the ^{18}O case the convergence of expansion (17) is much slower, although such convergence clearly exists. The largest difference between the results of columns 5 and 6 of table 1, appears in the $\langle (5/2)^2; J=0 | V_{eff} | (3/2)^2; J=0 \rangle$ matrix element and represents only 4%. For this reason we consider only up to F_6 terms in the determination of the effective interaction.

It is well known (Brandow 1967) that due to the inclusion of folded graphs the operator H_{eff} defined by

$$H_{eff} = H_0 + V_{eff} \quad (19)$$

is not Hermitian. Following the procedure described by Brandow (1968) and Des Cloizeaux (1960), one can find a symmetric H_{eff} having the same eigenvalues in the space of two-particle states with the original non-symmetric H_{eff} . The two-body matrix elements of the symmetric operator H_{eff} for all (J,T) states of the $A=18$ system (Skouras and Varvitsiotis 1990a) are found

to be in remarkable agreement with Kuo's matrix elements (Kuo 1967) and with those obtained by Preedom and Wildenthal (1972). This agreement shows that our matrix elements obtained without the use of any adjustable parameters, may be suitable for shell model calculations in the beginning of the sd shell. A first test was done by using our interaction to determine the spectra of the $A=19$ and $A=20$ nuclei. The results of this shell model calculation are shown in figures 3 and 4 and are in reasonable agreement with experiment (Ajzenberg-Selove 1983).

As mentioned in the beginning of this paper, we also use our method to determine the effective three-body interaction in the space of $0\hbar\omega + 2\hbar\omega$ excitations. In the case of 0p shell the dimensions of the energy matrices are not extremely large (the biggest dimension is 1868). Hence, the quantities R_n are determined directly by matrix inversion. We use two types of two-body interactions. The first is the "Sussex" interaction of Elliot et al (1968) while the other is a G-matrix (Skouras and Varvitsiotis 1990b) derived from the Reid soft-core potential (Reid 1968). We distinguish the results obtained using these two interactions by $V_{eff}^{(S)}$ and $V_{eff}^{(G)}$ respectively. In table 2 we present the results for the matrix elements of the three-body effective interaction. In this table there are several three-body matrix elements with magnitude between 0.5 and 1 Mev. This notice suggests that three-body forces will have an important effect on the spectra of nuclei with several valence particles in the 0p shell. Actually, in the calculation of the spectra of the 0p shell nuclei we find (Skouras and Varvitsiotis 1990b) the three-body interaction to produce significant differences in the excitation energies. These differences are of the order of several Mev near the end of the 0p shell. We also observe that generally, the three-body effects bring the calculated spectra to closer agreement with experiment. This behaviour is clear in fig.5 where the spectrum of ^{10}B is shown. The introduction of the three-body component of V_{eff} pushes up for example the (1,0) state from 0.13Mev to 2.44 Mev and better agreement with experiment is obtained.

REFERENCES

- Ajzenberg F-Selove 1983 Nucl. Phys. **A392** 1
 Brandow B H 1967 Rev. Mod. Phys. **39** 771
 Des Cloizeaux J 1960 Nucl. Phys. **20** 321
 Elliot J P, Jackson A D, Mavromatis H A, Sanderson E A and Singh B 1968 Nucl. Phys. **A121** 241
 Krenciglowa E M and Kuo T T S 1974, Nucl. Phys. **A235** 171
 Kuo T T S and Brown G E 1966, Nucl. Phys. **85** 40
 Kuo T T S 1967 Nucl. Phys. **A103** 71
 Mavromatis H A and Skouras L D 1979 Nucl. Phys. **A326** 83
 Preedom B M and Wildenthal B H 1972 Phys. Rev. **C6** 1633

Reid R V 1968 Ann. Phys. 50 411

Skouras L D and Varvitsiotis J C 1990a Nucl. Phys. A513 239

Skouras L D and Varvitsiotis J C 1990b Nucl. Phys. A513 264

Table 1
Convergence of V_{\dots} in terms of additional folded graphs

ME	Number of folds [*]						
	0	1	2	3	4	5	6
¹⁶ O	-95.02						
¹⁷ O							
5/2	-1.448	-1.431	-1.432	-1.432	-1.432	-1.432	-1.432
3/2	4.508	4.543	4.542	4.542	4.542	4.542	4.542
1/2	-1.895	-1.783	-1.785	-1.787	-1.786	-1.786	-1.786
¹⁸ O							
5.5	-2.424	-2.132	-2.297	-2.192	-2.260	-2.215	-2.246
5.3	-2.119	-2.913	-2.381	-2.733	-2.501	-2.657	-2.549
5.1	-1.487	-1.476	-1.419	-1.467	-1.434	-1.456	-1.440
3.5	-2.971	-3.040	-3.030	-3.029	-3.031	-3.030	-3.031
3.3	-1.378	-1.158	-1.187	-1.191	-1.184	-1.189	-1.185
3.1	-1.088	-1.035	-1.039	-1.041	-1.039	-1.040	-1.040
1.5	-1.366	-1.278	-1.302	-1.288	-1.298	-1.291	-1.296
1.3	-1.168	-1.157	-1.098	-1.149	-1.113	-1.138	-1.120
1.1	-1.457	-1.545	-1.541	-1.544	-1.540	-1.543	-1.541

* Each column of results represents the total results up to that order.
For ¹⁶O and ¹⁷O the contribution of H_0 has been added in the column of F_0 .

Table 2
List of 3-body matrix elements

ME	$V_{ijj}^{(S)}$	$V_{ijj}^{(R)}$	ME	$V_{ijj}^{(S)}$	$V_{ijj}^{(R)}$	ME	$V_{ijj}^{(S)}$	$V_{ijj}^{(R)}$
1,1	0.518	0.624	6,8	0.219	0.155	12,12	0.307	0.213
1,2	0.054	0.129	6,9	0.208	0.101	12,13	0.085	0.026
1,3	-0.418	-0.268	6,10	0.489	0.385	12,14	-0.063	-0.030
1,4	-0.464	-0.264	7,7	0.128	0.194	13,13	0.032	0.121
1,5	-0.715	-0.172	7,8	-0.070	-0.076	13,14	0.726	0.320
2,2	-0.305	-0.387	7,9	0.278	0.300	14,14	0.239	0.464
2,3	-0.139	-0.385	7,10	-0.266	-0.137	15,15	-0.187	-0.064
2,4	-0.143	-0.105	8,8	0.071	0.050	15,16	0.167	0.113
2,5	0.296	0.406	8,9	-0.008	0.045	16,16	-0.371	-0.147
3,3	-0.646	-0.744	8,10	-0.163	-0.021	17,17	0.363	0.625
3,4	-0.017	-0.086	9,9	0.277	0.254	18,18	-0.060	0.032
3,5	0.364	0.568	9,10	-0.131	-0.023	18,19	0.023	0.019
4,4	0.895	0.916	10,10	0.273	0.309	18,20	0.175	0.052
4,5	-0.296	-0.101	11,11	-0.001	0.012	19,19	0.131	0.119
5,5	-0.839	-0.719	11,12	-0.083	-0.043	19,20	-0.209	-0.087
6,6	0.153	0.148	11,13	0.120	0.070	20,20	0.214	0.148
6,7	0.054	0.069	11,14	0.341	0.224	21,21	0.063	0.075

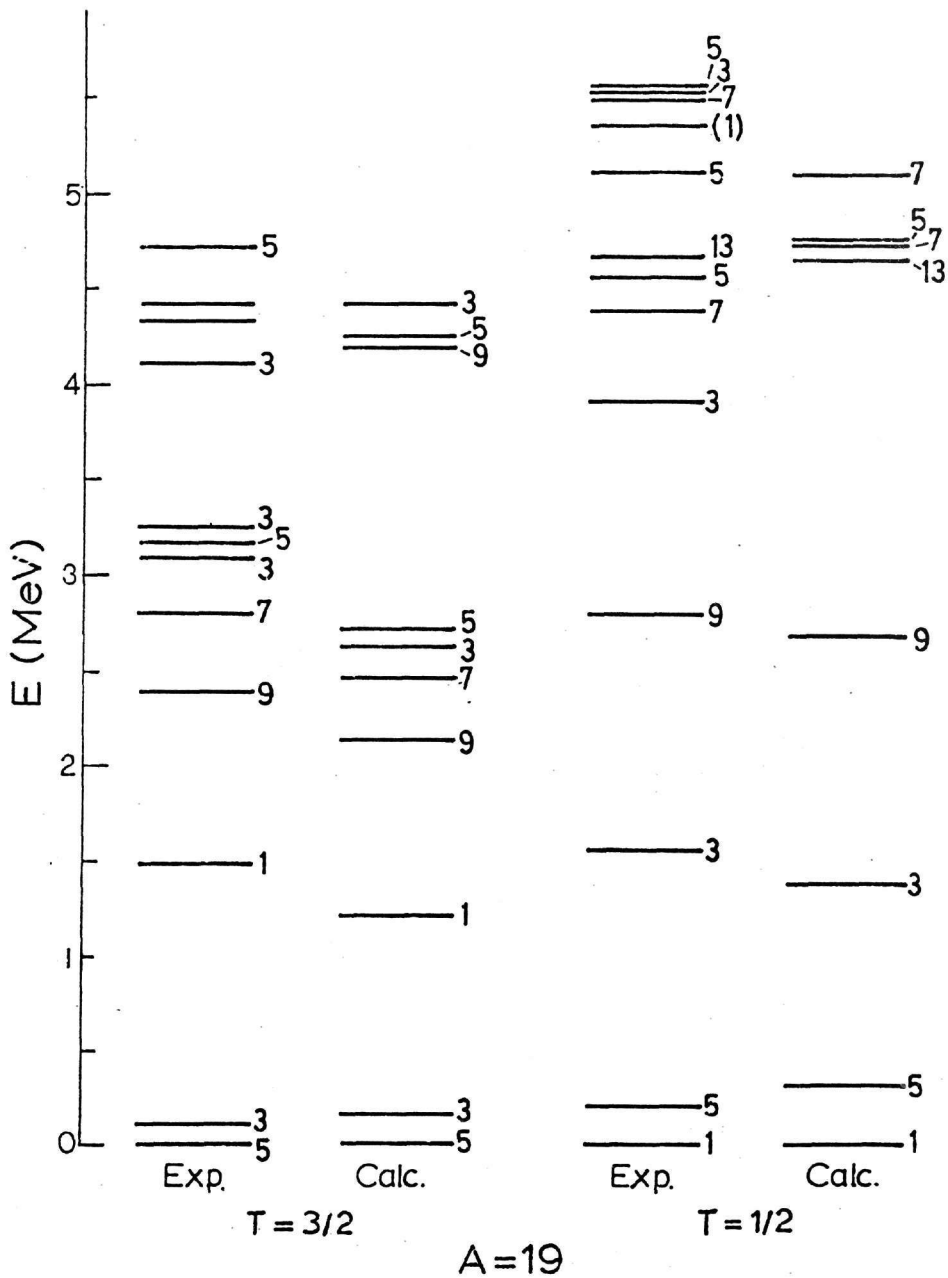


Fig.3. Energy spectra of the $A=19$ nuclei

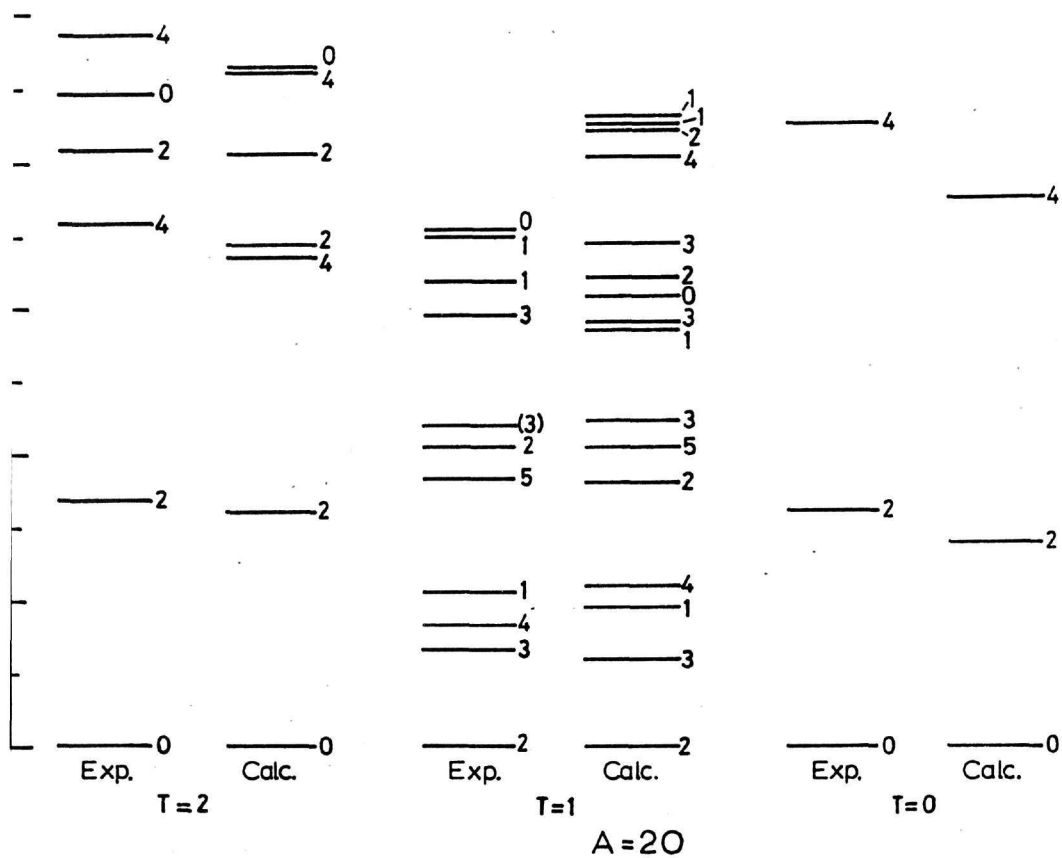


Fig.4. Energy spectra of the $A=20$ nuclei

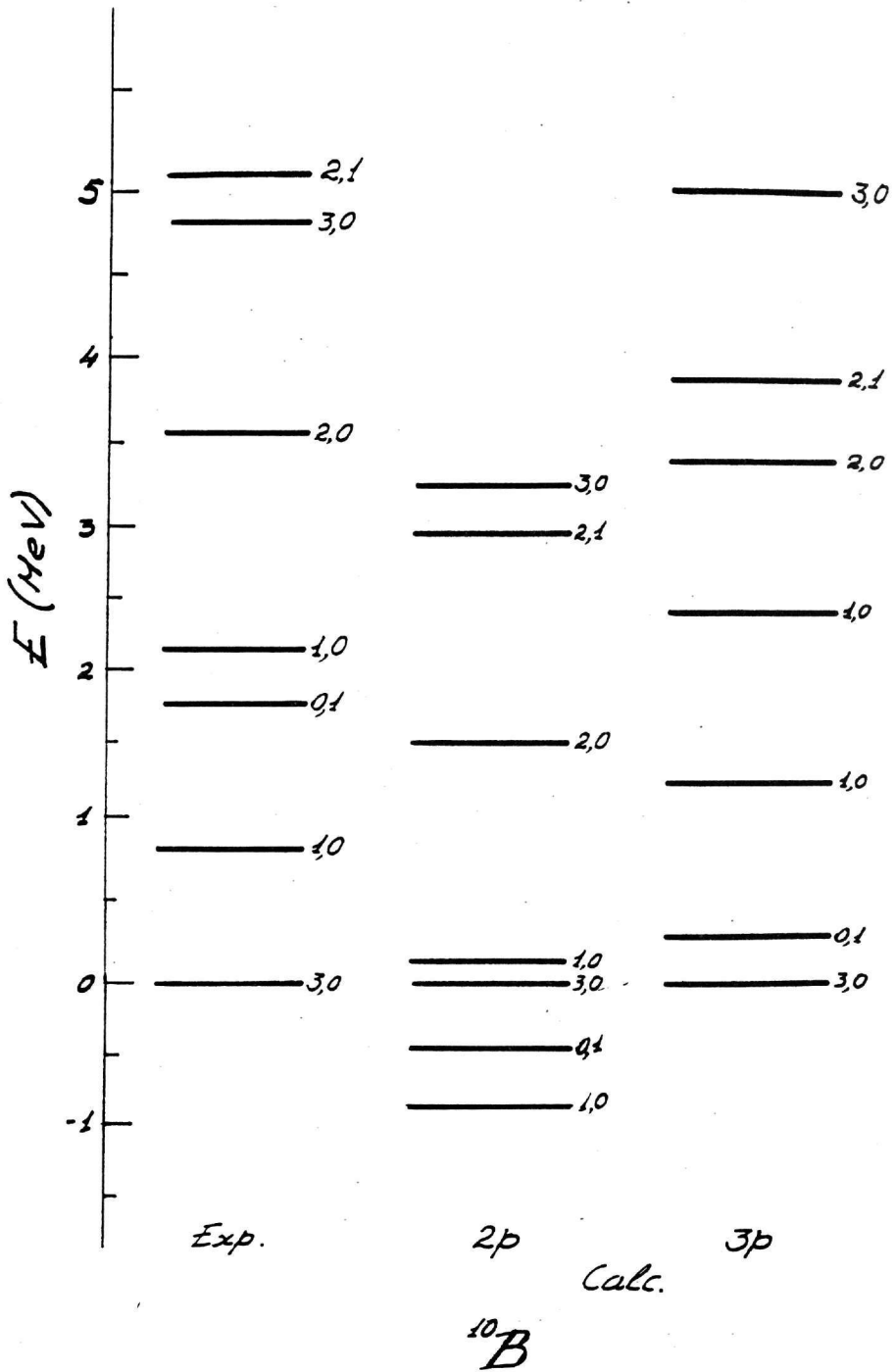


Fig.5. Energy spectrum of ^{10}B